ELSEVIER

Biochimica et Biophysica Acta 1326 (1997) 54–66

BIOCHIMICA ET BIOPHYSICA ACTA
BBA

Association of polyene antibiotics with sterol-free lipid membranes II. Hydrophobic binding of nystatin to dilauroylphosphatidylcholine bilayers

J. Milhaud [a,*], J. Berrehar [b], J.M. Lancelin [c], B. Michels [d], G. Raffard [e], E.J. Dufourc [e]

[a] *Laboratoire de Physicochimie biomoléculaire et cellulaire (UA CNRS 2056), Université Paris VI, B.P. 138, 75252 Paris Cedex 05, France*

[b] *Groupe de physique des solides (UA CNRS 17), Université Paris VI, Tour 23, 75252 Paris Cedex 05, France*

[c] *Institut de Biologie Structurale (CEA-CNRS), 41 Avenue des Martyrs, 38027 Grenoble, France*

[d] *Laboratoire d'Ultrasons et de Dynamique des Fluides Complexes (UA CNRS 851), Université Louis Pasteur, 67070 Strasbourg Cedex, France*

[e] *Centre de Recherche Paul Pascal (CNRS), 33600 Pessac, France*

Received 24 July 1996; revised 7 January 1997; accepted 13 January 1997

Abstract

Interaction of nystatin A_1 with multilamellar vesicles (MLV) of dilauroylphosphatidylcholine (DLPC), observed either by adding nystatin to preformed MLV (mixtures I) or by incorporating it during the formation of vesicles (mixtures II, inner lamellas of MLV in contact with nystatin) was investigated for $0.002 \leq \text{nystatin}/\text{DLPC} = R_A \leq 0.20$, by four complementary methods. The main results were: (i) Ultraviolet absorption and circular dichroism (CD) spectra of mixtures I revealed the occurrence of a saturable association with a stoichiometry ($R_A = 0.007 \pm 0.002$) constant between 3 and 33°C. (ii) By differential scanning calorimetry, thermograms of the two types of mixtures were similar only when water was in great excess. In the opposite (e.g., $(H_2O)/(\text{DLPC}) = R_W \leq 300$), mixture II thermograms displayed two features, upshifted by about 6.5°C with respect to the sharp peak observed with mixture I, resembling those obtained for pure DLPC when the low-temperature phase was the subgel phase. For this R_W, the nystatin absolute concentrations were those for which nystatin form superaggregates as revealed by the nystatin CD spectra. It is proposed that these superaggregates are excluded from the interlamellar spacings of MLV and exert a pumping action on the interlamellar water. The subsequent dehydration of the inner lamellas is thought to convert them into the subgel state. (iii) ^{2}H-NMR spectra of sn-2-perdeuterated DLPC MLV + nystatin mixtures II, confirmed such a temperature shift of the main transition. They showed, in addition, an ordering of the aliphatic chains immediately above the transition temperature, equivalent to a bilayer thickening of 2 Å.

Keywords: Deuterium nuclear magnetic resonance (^{2}H-NMR); Differential scanning calorimetry; Circular dichroism; Multilamellar vesicle; Nystatin A_1

Abbreviations: UV, ultraviolet; DSC, differential scanning calorimetry; CD, circular dichroism; NMR, nuclear magnetic resonance; MLV, multilamellar vesicles; LUV, large unilamellar vesicles; PC, phosphatidylcholine; DLPC, dilauroylphosphatidylcholine; DMPC, dimyristoylphosphatidylcholine; DPPC, dipalmitoylphosphatidylcholine; DMSO, dimethylsulfoxide; T_m, temperature of the main transition of phospholipids

* Corresponding author. Fax: +33 144 277560.

PII S0005-2736(97)00008-4

1. Introduction

Polyene antibiotics permeabilize sterol-containing natural and model membranes at low doses (antibiotic-to-phospholipid molar ratios, R_A, of typically ca. 10^{-4}) [1,2]. Their selective affinity for ergosterol leads to a specific permeabilization of membranes containing this sterol, like membranes of fungi, thereby conferring on them antifungal properties. Consequently, nystatin, like amphotericin B, is of wide use in human therapy. However, a major drawback of these antibiotics is their side activity towards the patient cholesterol-containing cell membranes. One of the methods used to reduce this side activity is to associate them with phospholipids (lipid formulations, e.g., Refs. [3,4]). In view of the development of such formulations, a better knowledge of the interaction of these antibiotics with liposomes containing exclusively phospholipids is desirable. Interaction of polyene antibiotics with sterol-free phosphatidylcholines membranes was proved to proceed as an actual binding from previous studies. By circular dichroism (CD*), it was established that amphotericin B and filipin bind to DMPC vesicles [5,6]; and it was demonstrated [6] that this process competes with the well-documented binding to membrane sterol. By ^{2}H-NMR, it has been revealed that the dynamics of DMPC acyl chains is modified in the presence of amphotericin B [7] and filipin [8]. On the other hand, it was observed that amphotericin B [5,9,10] and filipin [11] can induce a membrane permeabilization to alcaline ions, in the absence of any sterol, at a R_A of a few per cent. The relevance of this permeabilization to the antibiotic-altered lipid chain dynamics was proposed in the case of filipin [11].

From then on, we wanted to extend the scope of our investigations to nystatin. In order to identify, among several linear saturated 1,2-di-*n*-acyl PCs, the one which associates in the most stable way with nystatin, preliminary experiments by DSC and CD on mixtures with DPPC, DMPC and DLPC MLV were carried out [12]. They showed that it was the DLPC bilayers which associate with nystatin in the largest temperature range. This observation prompted us to undertake a thorough study of the interaction of nystatin with DLPC MLV, in spite of the ill-understood thermotropic behaviour of these vesicles [13–17].

In the present study, four complementary approaches were used: UV absorption and CD to follow the spectral changes of the antibiotic, DSC and ^{2}H-NMR to obtain information about the changes in the thermodynamic and dynamic state of the membranes, respectively.

2. Materials and methods

2.1. Materials

DLPC was purchased from Sigma (St. Louis, MO) and used without further purification. Nystatin A_1 was a generous gift from the Squibb Institute in a view of structural investigations [18]. As detected by UV absorption, it contains 3 mol% of heptaenic impurities. Preparation of aqueous nystatin solutions requires a previous dissolving in DMSO. The concentration of nystatin, when adding it as organic solutions, was deduced from their UV absorption ($\epsilon_{309} = 6.1.10^4$ M^{-1} cm^{-1} in DMSO and $\epsilon_{304} = 8.0.10^4$ M^{-1} cm^{-1} in methanol [19]). Because of its hygroscopicity, nystatin was stored in the presence of dry argon. The test of its preservation was the stability, in the dark, of the UV absorption of an aqueous solution after a 3-day incubation at 37°C. Three types of buffer were used. The low sensitivity calorimetric measurements were performed with a 100 mM phosphate (pH 7.2), buffer. CD and UV investigations were made with the same buffer, 10-fold diluted. For all the other experiments a 10 mM Hepes (pH 7.2), buffer was used.

For the CD and UV studies on aqueous nystatin solutions, a first 250-mM DMSO stock solution was made from which a second aqueous 2 mM stock solution was prepared and incubated overnight, at 5°C. Final aqueous solutions have a DMSO content lower than $0.5\ 10^{-4}$ v/v.

1-lauroyl-2-perdeuterolauroyl-sn-glycero-3-phosphocholine (sn-2-$^2H_{23}$DLPC) was purchased from Avanti Polar Lipids and controlled by TLC prior to use.

2.2. Lipid bilayers

The most thermodynamically stable form of lipid vesicles, namely MLV, was used. The desired amount

of phospholipid, as a chloroformic solution, was evaporated under a nitrogen flow. The dried film was desiccated for several hours in vacuum and dispersed in the buffer, with a bath sonicator, at room temperature, for 10 min. The lipid phosphorus content of the vesicles was determined according to Stewart [20].

2.3. Preparation of the antibiotic–lipid mixtures

Two modes of preparation were used. In mixture I, the desired amount of antibiotic in a DMSO solution was added to preformed MLV; the concentrations of these solutions were sufficiently high so that the proportion of added DMSO was smaller than 5% v/v. In mixture II, the antibiotic and the phospholipid were dissolved in methanol and in chloroform, respectively. The mixture was coevaporated, dried up under vacuum, and dispersed in the buffer. The obtained suspension was lyophilized. The resultant powder was finally hydrated, subjected to three thermal cycles through T_m, each cycle being followed by a mechanical shaking to ensure homogeneity. More specifically for NMR studies, before each cooling, a 30-min incubation at 40°C was performed and the hydration was carried out with deuterium-depleted water. In mixture II, nystatin is in contact with both sides of all the lamellas of each vesicle while, in mixture I, it is in contact only with the outer leaflet of the external lamella.

The antibiotic and the water contents of the mixtures were given by the antibiotic-to-phospholipid and the water-to-phospholipid molar ratios, R_A and R_W, respectively.

2.4. Spectroscopic measurements

For UV absorption, a Cary 1E spectrophotomer, equipped with a thermostated cuvette holder, was used.

The CD spectra were recorded with a Jobin Yvon Mark IV dichrograph, also equipped with a thermostated cuvette holder. $\Delta\epsilon$ is the differential molar dichroic absorption coefficient. Spectra were corrected for light scattering by vesicles.

2.5. Calorimetric measurements

High-sensitivity calorimetry experiments, at $R_W = 8.10^3$, were performed on a DASM-4 microcalorimeter [21], interfaced to a Bull Micral computer. Low-sensitivity calorimetry experiments, with $R_W = 220$, were performed on a Setaram DSC 111, interfaced to a Hewlett-Packard 86B. With both calorimeters, temperature was programmed only on heating. For each sample, at least two repetitive scans were carried out. To determine the enthalpy corresponding to an endotherm, a straight line was traced between its onset and its completion temperatures and the corresponding surface calculated with the software provided by MicroCal and Setaram respectively. When adding antibiotic as a DMSO solution, care was taken to add the same proportion of DMSO to the reference cell.

2.6. NMR measurements

The sample was enclosed in a 10-mm tube and placed in a Bruker MSL 200 NMR spectrometer operating at 30.7 MHz. Spectra were taken on decreasing temperatures and samples were allowed to equilibrate 30 min at a given temperature (regulated to ± 1°C) prior to signal acquisition. The quadrupolar echo sequence [22] was used with a 4 μs $\pi/2$ pulse, a 40 μs pulse spacing and 2 s recycling time. 2000 to 5000 acquisitions were performed per spectra on a 500 kHz spectral width. First moment calculation and spectral 'de-Paking' were performed as described elsewhere [23–25].

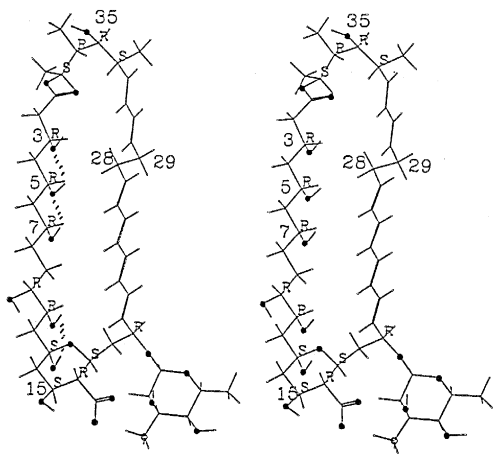

Fig. 1. Stereodiagram of a wire-type model of nystatin A_1. The atomic numbering corresponds to the one commonly used for nystatin [18,27,28]). Each asymmetric center is labelled with its absolute R/S stereochemistry. The structure is modeled with the 3, 5, 7 triol motif in an extended conformation.

2.7. Molecular modeling

Molecular modeling was done using the set of modeling programs from Biosym Technologies (San Diego, CA, USA). A molecular model of nystatin A_1 was constructed in vacuo within the BUILDER module of the program INSIGHT II. This model was made based on the cristallographic co-ordinates of amphotericin B [26] and the absolute stereochemistry of the structure [18,27,28] (see Fig. 1).

3. Results

3.1. Spectral characteristics of nystatin in the absence or presence of DLPC bilayers (mixtures I)

3.1.1. (A) Free nystatin

The CD spectra of nystatin aqueous solutions depended on the concentration. More generally, owing to the amphiphilic character of the polyene antibiotics, the hydrophobic polyene moieties tended to come together to be excluded from water and their interaction led to the appearance of an excitonic doublet [29]. In the case of nystatin, poorly reproducible CD spectra according to the incubation conditions were obtained if care was not taken to leave a concentrated (2 mM) aqueous stock solution incubate overnight from which final solutions were prepared. In these conditions, in a 10-mM phosphate buffer, only two CD spectra are obtained: (1) at concentrations lower than 15 μM a totally negative spectrum (data not shown); (2) at higher concentrations, a doublet with three negative bands at 323, 307 and 296 nm and a positive band at 276 nm (Fig. 2b). However, in a 100-mM phosphate buffer, a third CD spectrum appeared progressively from 250 μM which exhibit, at 5 mM, three positive bands at 321, 305 and 293 nm and three negative bands at 330, 315 and 276 nm (cf. Fig. 2a); we attributed it to a superaggregated state of nystatin. At these high concentrations, very small light path lengths (10^{-3} cm) were used in order to prevent any alteration of the CD spectra resulting from the high absorption [30].

The absorption spectra of nystatin aqueous solutions displayed a vibronic progression which did not depend on the concentration. However, from around 25 μM, as the solutions become more and more turbid, they no longer obeyed the Beer-Lambert law.

3.1.2. (B) Nystatin in the presence of DLPC bilayers

By adding preformed DLPC MLV to nystatin solutions (mixture I), UV and CD spectra were modified.

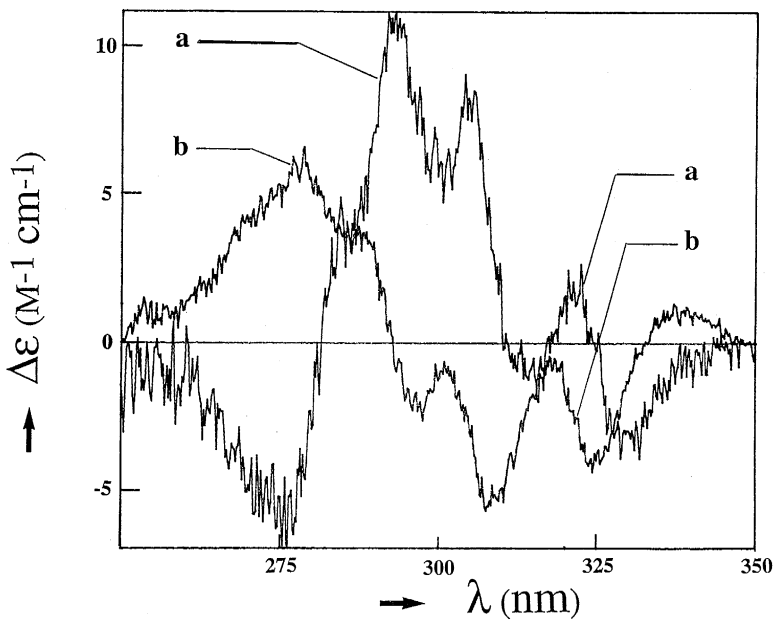

Fig. 2. CD spectra of buffered nystatin solutions (100 mM phosphate buffer, pH 7.2) with concentrations equal to 5 mM (a) and 80 μM (b).

In absorption, the contribution of the light scattering by MLV could be reduced by using the MLV suspension as a reference; resultant spectra were not too noisy until a DLPC-to-nystatin molar ratio of $1/R_A = 500$, owing to the very high nystatin extinction coefficient. As seen in Fig. 3A, the absolute and relative amplitudes of the bands of the vibronic progression changed in the presence of MLV. The apparent isobestic point at 330 nm was thought to be incidental as resulting from an additional light scattering of the mixtures with respect to nystatin-free suspensions due to the formation of big nystatin-MLV aggregates. Nevertheless, we postulated that, from the viewpoint of absorption, only two states of nystatin existed in the presence of MLV: the free and 'the bound species'. The extinction coefficient of 'the bound species', ϵ_B, was determined by incubating nystatin solutions, at concentrations for which the Beer-Lambert law applies (≤ 25 μM), with a large excess of DLPC MLV until the absorbance is steady: $\epsilon_B = 2.4 \times 10^4$ M^{-1} cm^{-1} at 306 nm. The concentration of the 'bound species' in the mixtures was calculated as [31]:

$$C_B = \frac{\epsilon_F l C_T - A}{\epsilon_F - \epsilon_B} \quad (1)$$

where C_T is the total concentration of nystatin, l the light path length, ϵ_F-$\epsilon_B = 2.8 \times 10^{-4}$ M^{-1} cm^{-1} at 306 nm and A the 306 nm absorbance of the mixture. For measuring this absorbance, a coarsely corrected baseline, obtained by linear extension of the background spectrum between 450 and 350 nm, was taken. From the results at 3°C, a binding isotherm was plotted (cf. Fig. 4), as a 'direct plot' [32]. It

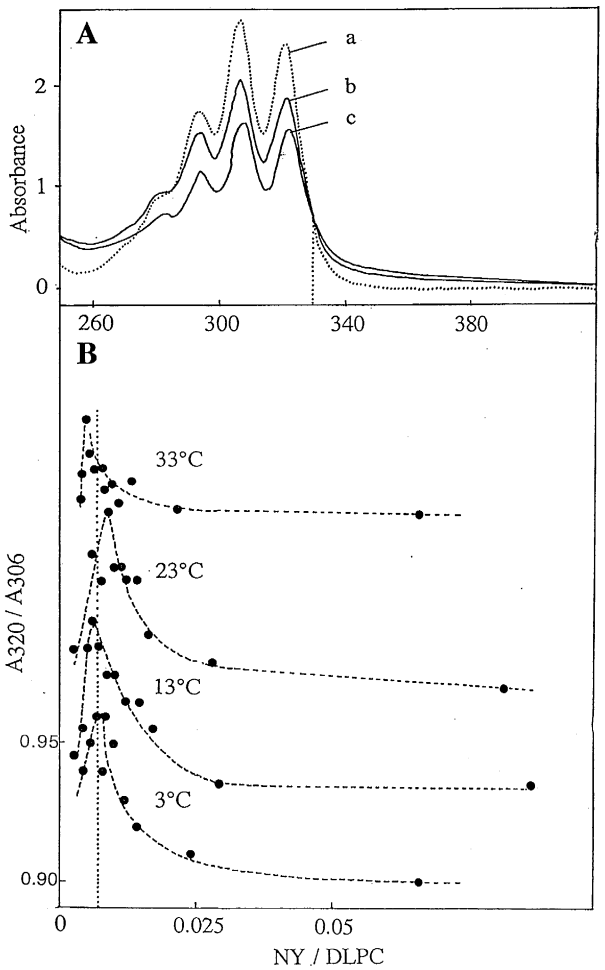

Fig. 3. (A) Absorption spectra of a 25 μM nystatin-buffered solution in the absence (a) and in the presence of preformed DLPC MLV with nystatin-to-DLPC molar ratios of 0.012 (b) and 0.0083 (c). (B) ratios of the 306 and 320 nm absorbances of mixtures corresponding to the titration of a 25 μM nystatin solution by cumulative additions of DLPC MLV at different temperatures. Plots for 13, 23 and 33°C are vertically displaced to show details of each plot, by keeping the same vertical scale as for 3°C. Maxima appear for nystatin/DLPC = 0.007 ± 0.002.

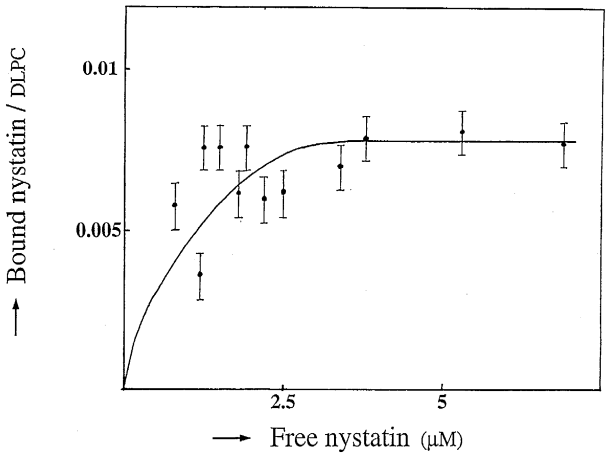

Fig. 4. Isotherm of binding of nystatin (≤ 25 μM) with DLPC MLV, at 3°C. The bound nystatin concentrations were calculated from the change of the 306 nm absorbance in the presence of MLV and the difference of the extinction coefficients of free and bound nystatin, ϵ_F-$\epsilon_B = 2.8$ 10^4 M^{-1} cm^{-1} at 306 nm (cf. text); free nystatin concentrations were obtained by difference. Care was taken to preserve the samples from an irradiation inside the cuvette-holder because of the long delay for reaching the equilibrium (~ 8 h). Only vertical error bars were traced for clarity.

clearly showed a saturation plateau at bound nystatin/DLPC = 0.008 ± 0.0015.

As a confirmation of a well-defined stoichiometry for the association, a titration of a 25-μM nystatin solution by cumulative additions of MLV was performed. The corresponding changes of the relative amplitudes of the bands of the vibronic progression were followed. In these experiments, our analysis was based on the principle that if a spectral parameter, characteristic of mixtures of two components A and B, goes through a maximum by varying the stoichiometric molar ratio A/B, the A/B value corresponding to this maximum represents the stoichiometric ratio of their association ('mole ratio method', cf. Ref. [33]). The selected parameter was the ratio of 306 and 320 nm absorbances. As shown in Fig. 3B, the ratio of these absorbances went through a maximum when decreasing R_A, at the same value, R_A = 0.007 ± 0.002, at 3, 13, 23 and 33°C, which indicated that the stoichiometric ratio at saturation did not vary between 3 and 33°C.

In contrast with absorption in CD, the extinction coefficient of nystatin was low: after substraction of the light-scattering by MLV from the CD spectra of mixtures, the noise was important from $1/R_A = 50$. Nevertheless, we could follow the transformation of the CD spectrum of aggregated nystatin (80 μM), by adding DLPC MLV. At first, the negative bands were blue-shifted by 5 nm (data not shown) and then were replaced by two positive bands at 278 and 323 nm. The amplitude of the latter band went through a maximum at $1/R_A(\text{sat}) = 130 \pm 20$ (data not shown). This stoichiometry was about the same as the one obtained, from absorption measurements, for monomeric nystatin.

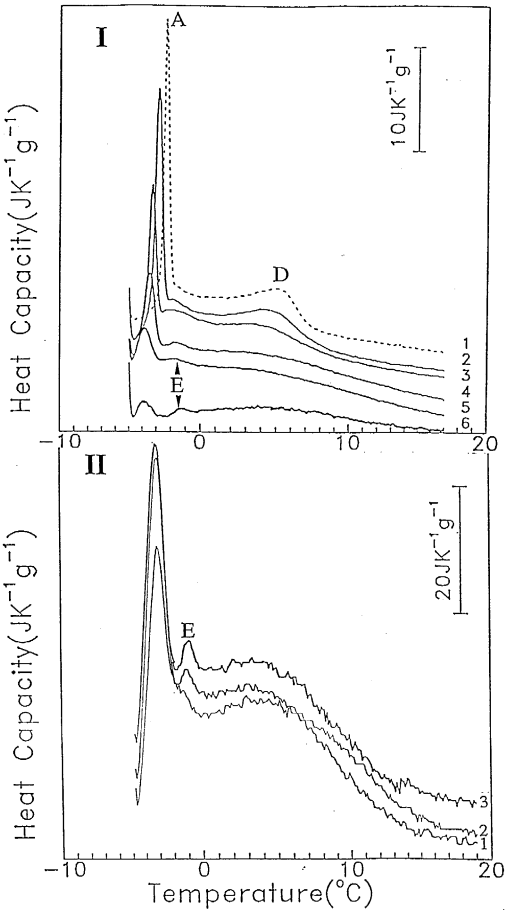

Fig. 5. High-sensitivity DSC recordings (H_2O/DLPC = 8 10^3, sample weight: 0.9 mg, heating scan rate 0.25°C/min). (I) Thermograms of mixtures II (cf. Section 2) with different nystatin-to-DLPC molar ratios, R_A; 1: $R_A = 0$; 2: $R_A = 0.0045$; 3: $R_A = 0.0091$; 4: $R_A = 0.040$; 5: $R_A = 0.10$; 6: $R_A = 0.18$. Thermograms are vertically displaced in order to show the details of each one. (II) Thermograms of mixtures I (cf. Section 2), with $R_A = 0.20$, for three heating scans numbered in successive order.

3.2. Physical state of membranes in the presence of nystatin (mixtures I and II)

3.2.1. (A) Thermal behaviour of mixtures when water is in large excess ($R_W = 8.10^3$)

High-sensitivity calorimetry experiments, on pure DLPC MLV and mixtures I and II very diluted (DLPC ~ 7 mM), were performed at a 0.25°C/min heating rate, from −5.5°C; no additive was introduced to prevent the freezing.

The pure DLPC, thermograms were characterized by a sharp peak, A, at −2.4°C and a broad maximum, D, around 4.5°C (cf. Fig. 5I,1).

The thermograms of intimate mixtures II (cf. Methods) differed from the previous ones by the two following points (cf. Fig. 5I,2 to Fig. 6):

(1) On increasing R_A, the temperature interval between the limits of the global endotherm was enlarged. The maximum of A, T_{max}, was taken as the lower limit of the endotherms because the minimum preceding A is not physically significant (the calorimeter has not reached its equilibrium yet); it decreases on increasing R_A. At the same time, a

small feature *E* appeared at an approximately constant temperature of −1.7°C, whose surface increases, with respect to *A* one, with R_A (e.g., compare Fig. 5I,6 and Fig. 5I,5). The higher limit, T_{compl}, corresponded to the intersection between the falling edge of D and the baseline; it increases with R_A. Both limits have been plotted against R_A, in Fig. 6, as a tentative of a 'phase diagram' representation [34], by considering coarsely that T_{max} and T_{compl} of pure DLPC, lumped together, represent the DLPC 'chain-melting transition temperature'. On each side of this 'transition temperature', were a fluid phase and a 'solid' phase whose identifications will be discussed further.

(2) On increasing R_A, *A* and *D* features were flattened. The corresponding enthalpies, ΔH_D and ΔH_A, have been arbitrarily calculated by drawing linear baselines from the minimum between A and E, tangentially to the final baseline and to the minimum preceding the A peak. When increasing R_A, ΔH_A exhibited a biphasic decrease (cf. Fig. 7) while ΔH_D stayed approximately constant.

For less intimate mixtures I, it is worth noting that the small endotherm *E*, not always present at the first scan, systematically increased by repeating scans, as shown in Fig. 5II,1,2,3.

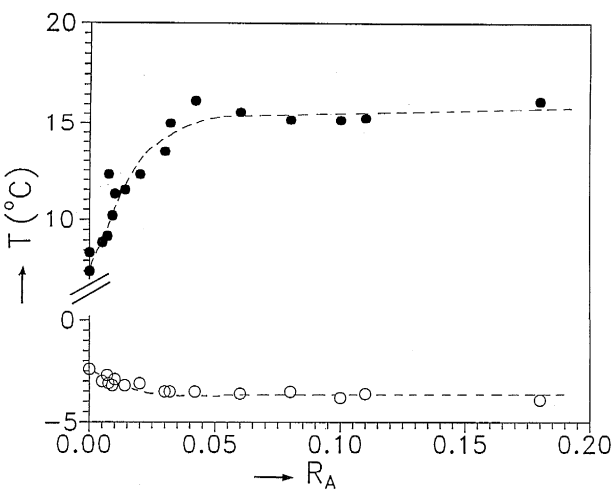

Fig. 6. Variations against the nystatin-to-DLPC molar ratio, R_A, of the low and high temperature limits, T_{max} (○) and T_{compl} (●), of the global endotherms of mixtures approximated to 'liquidus' and 'solidus' lines [34]. From the upward curvature of the first, compared with the flatness of the second, it is inferred that nystatin is miscible most solely with the DLPC fluid phase.

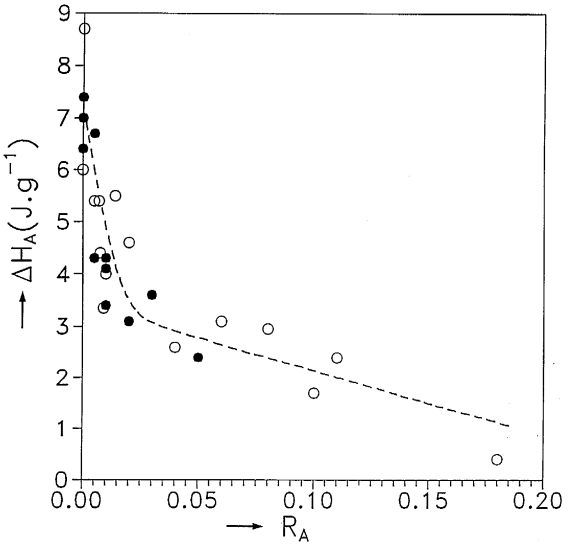

Fig. 7. Variation of the enthalpies, ΔH_A, of the sharp peak A of mixtures II thermograms (cf. Section 2), against the nystatin-to-DLPC molar ratio, R_A, at two water-to-DLPC molar ratio, R_W. (○): $R_W = 8.10^3$; (●): $R_W = 220$.

3.2.2. (B) Thermal behaviour and dynamic properties of the mixtures when water is in small excess

3.2.2.1. ^{2}H-NMR study on intimate mixtures II (R_W = 380). Deuterium solid state NMR spectra of DLPC were recorded, on decreasing temperatures from 60°C to −20°C, in the absence and the presence of various amounts of nystatin (R_A = 0.005, 0.05, 0.20, 0. 50). Selected spectra are shown in Fig. 8. Pure lipid spectra (left column, A) exhibited an axially symmetric line shape at 0°C and above, indicating that the system was in the fluid, L_α, state. The rigid limit pattern observed at −10°C indicated that the molecular motions were totally frozen, as in the gel, $L_{\beta'}$, phase. Addition of nystatin (middle and right columns, B and C) was reflected by an upshift of the temperature at which the fluid phase spectra were observed. Interestingly, this shift was observed for very low nystatin doses and did not seem to increase when R_A is higher than 0.05. Fluid phase spectra were quasi-identical for corresponding temperatures in the presence or absence of antibiotic. Calculation of the first spectral moment, M_1, [22] allowed to better quantitate the thermal variations of spectra. Resulting M_1 values are plotted in Fig. 9, as a function of tempera-

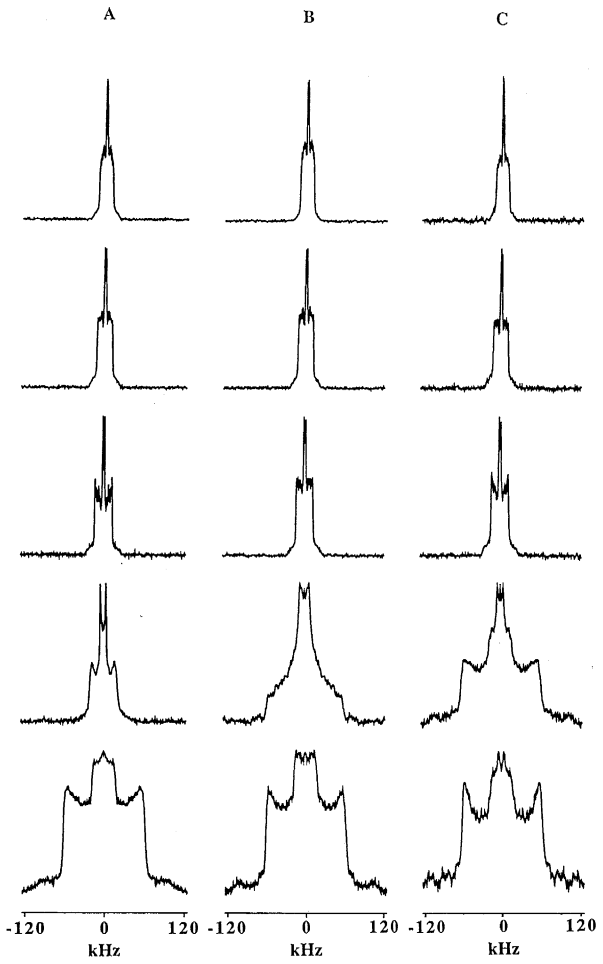

Fig. 8. Selected solid state ^{2}H-NMR spectra of (sn-2-$^2H_{23}$) DLPC/water dispersions in the absence (A) and the presence (B, $R_A = 0.005$; C, $R_A = 0.2$) of nystatin. Temperatures decrease from top to bottom as 60°C, 40°C, 20°C, 0°C, −10°C.

ture, for two nystatin contents ($R_A = 0.005$ and 0.2); values for $R_A = 0.05$ and 0.5 overlapped with those for $R_A = 0.2$ and were not plotted for clarity. It was clearly seen that the transition temperature, associated with chain disordering, occurred at ca. −2.5°C for pure bilayers, in agreement with Morrow and Davis [13] when they performed experiments on decreasing the temperature. In the presence of the antibiotic, the transition was shifted upwards increasingly with the drug content, namely to ca. 0°C for $R_A = 0.005$ and ca. 3°C for $R_A \geq 0.05$ (cf. Fig. 9). M_1 values were about the same for temperatures above 30°C, indicating that nystatin, even at high doses, e.g., $R_A = 0.5$, did not perturb the chain ordering in these conditions.

For temperatures below the phase transition, it was difficult to quantitate small variations in ordering due to intrinsic experimental error in M_1 determination (ca. 5%). One can only mention that M_1 values in the absence or the presence of nystatin were very high, demonstrating that the DLPC chains were highly ordered. In the fluid phase, M_1 values could be used to calculate the bilayer hydrophobic thickness, d_h, [35,36]. For the pure system, at 5°C, $d_h = 21.2$ Å. Addition of nystatin with $R_A = 0.2$ increases it by ca. 2 Å. Therefore, and at converse to high and low temperatures, the antibiotic appeared to order the system just above T_m. This was further investigated by de-paking powder patterns. Such 'oriented-like' spectra depicted the minute variation of the orientational ordering along the fatty acyl chain (not shown). In the presence of nystatin, a general ordering effect was perceived for all deuterium-labeled positions with a marked increase for positions near the bilayer center. At 10°C these effects were already maximum for $R_A = 0.005$. At 5°C, i.e., closer to the order-disorder transition, the ordering induced by the antibiotic was even more effective. In addition, all the lines got broader in the presence of nystatin which reflected the onset of slow motions.

3.2.2.2. Low-sensitivity calorimetry on mixtures I and II ($R_W = 220$). Measurements were performed at a 0.2°C/min heating rate from −5°C, without additive

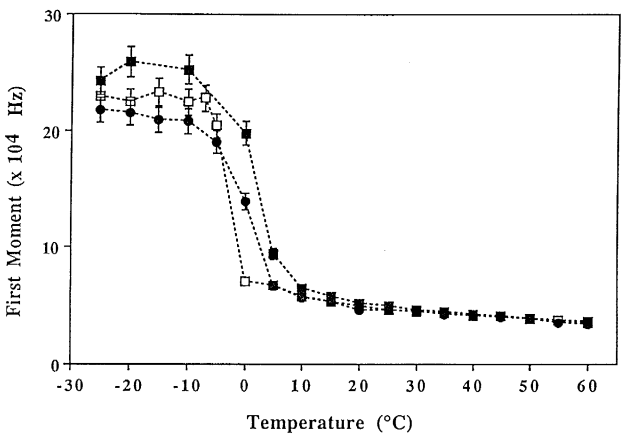

Fig. 9. Temperature dependence of the first moment of (sn-2-$^2H_{23}$) DLPC spectra in the absence (□) and the presence (●, $R_A = 0.005$; ■, $R_A = 0.2$) of nystatin. Values for $R_A = 0.05$ and 0.5 overlap with those for $R_A = 0.2$ and were not plotted for clarity. Dotted lines are only drawn as eye guides.

to the buffer to prevent the freezing; no prolonged incubation at the starting temperature was made.

For pure DLPC MLV, the thermograms were identical to those obtained with $R_W = 8\ 10^3$ (Fig. 10I).

In the presence of nystatin, the thermograms depended on the mixture preparation mode. For mixtures I (nystatin in contact only with the outer lamella of MLV), A and D merely flattened (cf. Fig. 10II), like for $R_W = 8.10^3$; at variance, for mixtures II (nystatin in contact with all the lamellas of MLV) two new features, B and C, appeared at 3 and 4.8°C respectively (Fig. 10III). These new features were poorly separated and could mask a remaining flattened D feature. Enthalpies of the features of mixtures I and II thermograms were reported in Table 1. The global enthalpies at each nystatin content (the sum of the numbers in the 2nd and 3rd columns of Table 1) were equal for the two mixtures, in the accuracy of measurements (± 0.3 kJ mol^{-1}). However, ΔH_A was smaller for mixture II than for mixture I, while the global enthalpy of B and C is higher than ΔH_D. Let us note that the small feature *E*, observed at $R_W = 8.10^3$, also appeared at $R_W = 220$ (cf. Fig. 10II,III).

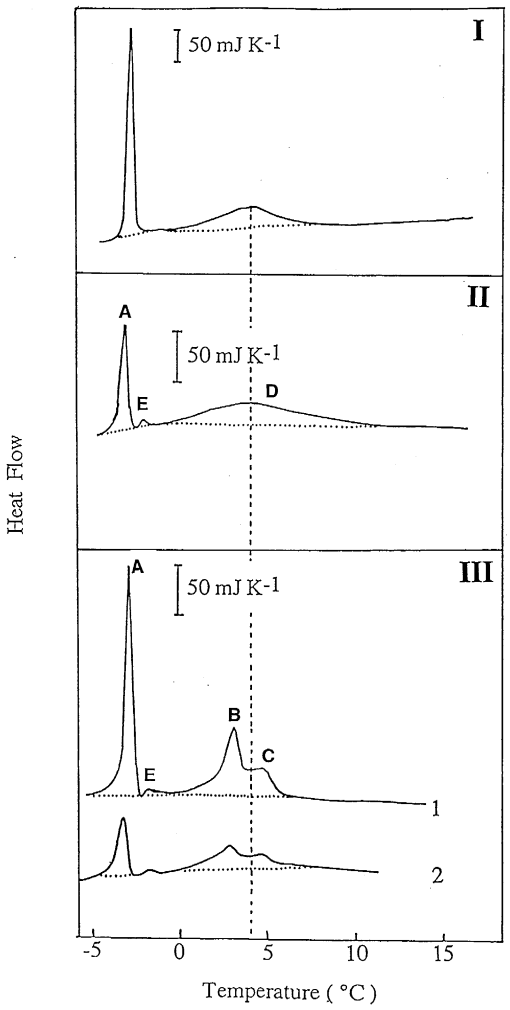

Fig. 10. Low-sensitivity DSC recordings (H_2O/DLPC ~ 220, sample weight: 15 ± 2 mg) of: pure DLPC MLV (I); a mixture I (cf. Section 2) with $R_A = 0.019$ (II); mixtures II (cf. Section 2) with $R_A = 0.005$ (1) and $R_A = 0.019$ (2) (III).

Table 1
Enthalpies, in J g^{-1}, corresponding to the different features of the thermograms obtained by low-sensitivity calorimetry (cf. Fig. 10II and III). The accuracy of measurements is ± 0.3 J g^{-1}

Nystatin-to-DLPC molar ratio, R_A	Enthalpy of the A feature	Enthalpies of (II): the B and C features (I): the D feature
0.005	3.3 (I) [a]	1.2 (I)
	2.2 (II) [a]	2.6 (II)
0.01	3.3 (I)	1.7 (I)
	2.6 (II)	1.6 (II)
0.019	2.8 (I)	2.5 (I)
	2.0 (II)	3.4 (II)
0.03	2.6 (I)	1.4 (I)
	2.2 (II)	1.7 (II)
0.05	2.5 (I)	1.6 (I)
	1.5 (II)	3.7 (II)

[a] I and II designate the two preparation modes of the mixtures (cf. Section 2).

4. Discussion

The results show that nystatin associates with fluid DLPC membranes in an extended temperature range, and that the subsequent change of the thermodynamical state of the membranes depend on the water content. In the following, the behaviours of the antibiotic and the membranes during the interaction will be separately discussed.

4.1. Interaction as viewed by the antibiotic (UV and CD investigations)

From the appearance or not of a horizontal asymptote on the binding isotherm [32], it can be discrimi-

nated between a mere partitioning of the antibiotic between the aqueous and membranous phases and an actual binding to saturable sites. Generally, in the binding of a ligand L to a substrate S bearing n independent sites per molecule having the same microscopic constant of binding, k, the average number of ligand molecules bound to one molecule of substrate, is [32]:

$$\bar{i} = \frac{\sum_{i=1}^{n} i[SL_i]}{[S_{tot}]} = \frac{nk[L]}{1 + k[L]} \quad (2)$$

where $[L]$, $[S_{tot}]$ and $[SL_i]$ are the concentrations of the free ligand, the total substrate and the association of i ligand molecules with one substrate molecule. Our binding isotherm at 3°C, with an asymptote of 0.008 ± 0.0015 (cf. Fig. 4), can be fitted to Eq. (2) by postulating that nystatin (the ligand) bears $1/0.008 = 130$ interaction sites. Such a stoichiometry is confirmed by the value of R_A for which the ratio of 320 and 306 nm absorbances goes through a maximum: R_A (sat) $= 0.007 \pm 0.002$, whatever is the temperature between 3 and 33°C (cf. Fig. 3B). Is such a number of DLPC molecules in interaction with one nystatin molecule realistic? Some preliminary microscopic observations (J. Milhaud, unpublished data) have led us to think there is a demixing of the nystatin-containing suspensions with formation of aggregates in which almost all the bound nystatin molecules would be entrapped. How could the molecular organization in such aggregates be envisaged? The aggregation of non-compressible vesicles leaves free spacings whose volumes are similar to the volume of one vesicle. We will model it as a stacking of cubic vesicles (0.3 μm edged cubes), delimiting cubic cavities, in the same number, which contain nystatin. The volume fractions occupied by each type of cubes are the same and the stoichiometric ratio at saturation will be locally preserved. If nystatin is entirely contained in such cavities, its concentration will be locally increased by a factor equal to the inverse of this volume fraction. To evaluate it, we will take, as an example, a mixture with an average nystatin concentration of 100 μM. The corresponding DLPC concentration, by supposing that it is entirely bound, is 13 mM. We will take for the surface by DLPC polar head in a lamella, 70 A^2, and for the proportion of DLPC molecules contained in the outer lamella of vesicles, 40% (cf. further). In these conditions, the number of DLPC molecules per vesicle is 4.10^6, the number of vesicles per ml is 2.10^{12} and the volume fraction corresponding to the DLPC-containing cubic vesicles 5%. Since the volume fraction occupied by nystatin-containing cubic cavities is the same, the local nystatin concentration will be higher than the average one by a factor of 20. Thereby, the strong osmotic gradient from inside to outside of aggregates makes the conservation of MLV integrity hardly probable. However, in these confined spacings, it is not unrealistic to envision an interaction of one nystatin molecule with 130 DLPC molecules through a network of H bonds connecting the OH groups of nystatin molecule with the polar heads of DLPC.

This stoichiometry can be compared with the results of two groups of authors making use of the intrinsic fluorescence of nystatin to study its interaction with DMPC [37] and DPPC [38] vesicles. By increasing the phospholipid molar ratio, $1/R_A$, both obtained an increase of the quantum yield with a saturation effect for values in the same order of magnitude as our stoichiometric ratio at saturation ($500 < 1/R_A < 1000$). It is worth noting that this $1/R_A$ value is compatible only with a localization of nystatin at the interface of vesicles, at variance with the interpretation of both groups of authors [37,38].

4.2. Interaction as viewed by the membrane (DSC and ^{2}H-NMR investigations)

By DSC, our pure DLPC thermograms exhibit reproducibly, for $R_W = 220$ as well as for $R_W = 8.10^3$, a sharp peak at -2.4°C (A) and a broad maximum around 4.5°C (D) (cf. Fig. 5I,1 and 11I). Several groups of authors investigated the thermal behaviour of DLPC bilayers by using different methods: DSC [13–15], RX diffraction [16] and ^{2}H-NMR [13,17]. From these studies the behaviour of DLPC bilayers differ from that of bilayers of saturated 1,2-di-*n*-acyl PCs with longer chains ($n \geq 14$). It depends on the hydration and the thermal history of the sample. At $R_W = 350$ and without annealing at low temperature [15], thermograms displayed two features similar to A and D ours. In contrast, at

$R_W = 75$ and after annealing 6 h below 0°C, thermograms displayed two other features with maxima at 3 and 4.5°C [13,14]. They are similar to B and C of our mixture II thermograms for $R_W = 220$. These differences indicate the participation of phases different from the ones involved in the order (gel phases $L_{\beta'}$ or $P_{\beta'}$) to disorder (fluid phase L_α) chain-melting transition of diacyl PCs with longer chains. Concerning the low-temperature phase, it was established [14] that the $L_{\beta'}$ and $P_{\beta'}$ gel phases become increasingly unstable with respect to the subgel phase L_c, with decreasing the length of the acyl chains. Concerning the high-temperature phase, the existence of an unusual fluid phase, L_x, partially disordered, was inferred from a R.X. diffraction study [16]; the feature *D* was then assigned to the L_α to L_x transition. A confirmation of the above interpretations was recently obtained by a ^{2}H-NMR study at high pressures [17]. The results obtained in these conditions indicate that L_x and L_c are the high and the low-temperature phases respectively, involved in the transition, provided that the thermodynamical equilibrium is reached. Now, reaching this equilibrium requires special conditions (a cooling rate smaller than 0.01°C/min or a prolonged stay below 0°C). These conditions are not fulfilled as often as the feature *A* appears (cf. [15] and present experiments). Consequently, it may be postulated that the presence of *A* on thermograms reflects the existence of a metastable gel phase ($P_{\beta'}$ or $L_{\beta'}$); conversely, the appearance of *B* and *C* would reflect that of L_c. This assumption seems supported by Morrow and Davis result of a reappearance of *A*, in addition to *B* and *C*, when supplementary water was added to preformed MLV without additional cold incubation [13]. This result was attributed to a non-equilibrium hydration between the outer lamella of MLV and the inner ones [13]; this interpretation supposes that the different lamellas of one MLV could give rise to different features and that the appearance of *B* and *C* would correspond to a low-temperature phase less hydrated than that corresponding to *A*.

Keeping in mind these data on pure DLPC, let us consider the effect of nystatin on thermograms. Our main result is that, for $R_W = 220$, the mixture II thermograms exhibit *A*, *B* and *C* features observed on the latter Morrow and Davis thermograms [13]. On the other hand, our mixture I thermograms exhibit the *A* and *D* features observed by Finegold et al. [15]. Nevertheless, the global enthalpies at each nystatin content are approximately the same in both cases (cf. Table 1). Consequently, we think that the increased complexity of mixture II thermograms, with respect to mixture I ones, is due to the presence of nystatin in the interlamellar water. Let us recall that, for this R_W value, the absolute nystatin concentrations (5 mM for $R_A = 0.02$) are those for which the nystatin CD spectra revealed the existence of a superaggregated state. These superaggregates, in equilibrium with the monomer, could be partially excluded from the interlamellar spacings because of their bulkiness. The subsequent upsetting of the equilibrium with the monomeric nystatin in the interlamellar spacings could lead to a pumping effect on the interlamellar water. A similar dehydration mechanism was described for another macromolecule, the soluble polymer polyethyleneglycol [39]. A dehydration of inner lamellas could specifically modify their thermodynamical state. This could lead to an increase of their transition temperature, displayed as *B* and *C* features on thermograms. We will now discuss our ^{2}H-NMR results obtained with a similar water content ($R_W = 380$). In the presence of nystatin occurs an upshift in temperature (5.5°C at $R_A = 0.05$, cf. Fig. 9) of the drop of the first spectral moment on heating, reflecting an upshift of the chain-melting temperature for the most of MLV lamellas. It agrees reasonably with the interval between the average temperature of *B* and *C* and that of *A* on thermograms (6.5°C). So, we propose that *B* and *C* correspond to the transition of the inner lamellas of MLV and *A* to the one of the outer lamella. This interpretation is near to that of Morrow and Davis. As, on pure DLPC, the appearance of *B* and *C* reflects the occurrence of L_c as the low-temperature phase, it might be then postulated that the introduction of nystatin into the interlamellar spacings would be sufficient to induce the formation of L_c, at small water content, in the absence of any annealing at low temperature.

Another interesting DSC result is the increase in surface of the small endotherm *E*, on the mixture I thermograms at $R_W = 8.10^3$, when repeating scans, (cf. Fig. 5II1,2,3). As mixture I is less intimate than mixture II, this suggests that *E* is related to the thermodynamic equilibrium. As the *E* surface in-

creases with R_A, with respect to the A one (cf. curve 6 on Fig. 5I), we tentatively attribute E to the chain-melting transition of nystatin-DLPC aggregates. This interpretation implies that the DLPC-nystatin association results in macroscopically separated entities; preliminary microscopic observations authorize such an interpretation (J. Milhaud, unpublished data).

On Fig. 7, on increasing R_A, ΔH_A exhibits a biphasic decrease at $R_W = 220$ as well as at $R_W = 8.10^3$. The significance of such a behaviour can be appreciated by paralleling DSC and ^{2}H-NMR results. At very small R_A ($R_A = 0.005$), ΔH_A experiences an important drop, while a noticeable chain ordering is revealed by an upshift of the temperature of the abrupt change of the first spectral moment, M_1, of ^{2}H-NMR spectra (cf. Fig. 9). From $R_A = 0.02$, ΔH_A decreases more slowly and the temperature of the M_1 change stays approximately constant at $T_m + 5.5°C$. So, it clearly appears that, in the interval between 0.005 and 0.02, a critical R_A-value occurs on each side of which the nystatin effect is qualitatively different. We relate this value to the stoichiometry of the DLPC-nystatin association in mixture II. As a matter of fact, for mixtures II, the number of sites of interaction per vesicle and consequently R_A(sat) is higher than that for mixture I; let us note that if 40 mol% of lipids are contained in the outer lamella of our MLV, the only one accessible to nystatin for mixture I, the stoichiometry at saturation for mixtures II would be increased from 0.007 to 0.017.

In Fig. 6, the variation of T_{compl} as a function of R_A, which can be approximated to a 'liquidus' line [34], exhibits an important upward curvature. Conversely, the variation of T_{max} as a function of R_A, which can be approximated to a 'solidus' line, is essentially flat. It can be inferred that nystatin is miscible almost solely with the fluid DLPC.

In conclusion, it can be stated, from the antibiotic viewpoint, that: (1) the association of nystatin with DLPC membranes is saturable and stable within a broad temperature range; (2) the stoichiometry precludes a localization of nystatin inside the membranes. A different situation was observed for another polyene antibiotic, filipin, for which the calorimetric results are compatible with a penetration of filipin into membranes [40]. The different behaviour of nystatin could arise from its stereostructure. As shown on the molecular model of Fig. 1, it differs from that of its homologue amphotericin B [26] by two items: (1) the polyol C_1-C_{12} chain is organized with a syn 3,5,7-triol pattern which, according as the surrounding medium is polar or apolar, gives rise to a mixture of gauche/trans conformers or to a well-defined extended conformation by the formation of intramolecular hydrogen bonds [28]; (2) the saturated C_{28} and C_{29} carbons disrupt the conjuguated polyene moiety into tetraene and diene fragments. These ones are not in the same plane, thereby allowing bent conformations. Such conformations seem not easily compatible with a penetration into membranes, in the absence of sterol. From the membrane viewpoint, the DLPC bilayers undergo an ordering of their fatty acyl chains even at very small nystatin doses ($R_A = 0.005$). This ordering effect differs from those previously reported for amphotericin B [7] and filipin [8] on DMPC bilayers; these latter promoted only the formation, above T_m, of membrane domains of very restricted dynamics (gel-type phases) in slow exchange with the 'non-complexed' lipids, not significantly modified [7,8]. Concerning the interaction with other phospholipid bilayers, a systematic study by DSC of the effect of filipin and nystatin on saturated 1,2-di-*n*-acyl PCs where $n = 12$, 14, 16 and 18 [12], showed that the sharp endotherm at T_m corresponding to the main transition of the pure phospholipid was replaced by a broadened endotherm extended towards high temperatures. Consequently, it can be said that these antibiotics induce an increase in order of the fluid lipid chains. Similarly, amphotericin B promotes on MLV of saturated and unsaturated phospholipids an upshift of the midpoint transition temperature [41,42]. So, it appears that the ordering action of polyene antibiotics upon the lipid chains of phospholipid bilayers could be a general consequence of their association with fluid bilayers.

Acknowledgements

The first author is indebted to Prof. K. Ohki and Japan Society for the Promotion of Science for having allowed preliminary DSC measurements, in Tohoku University, in Sendai (Japan). She thanks Dr. Ollivon for helpful discussions.

References

[1] Bolard, J. (1986) Biochim. Biophys. Acta 864, 257–304.
[2] Bolard, J., Legrand, P., Heitz, F. and Cybulska, B. (1991) Biochemistry 30, 5707–5715.
[3] Hiemenz, J.W. and Walsh, T.J. (1996) Clin. Infect. Dis. 22, suppl. 2, S133–144.
[4] Mehta, R.T., Hopfer, R.L., Mc Queen, T., Juliano, R.L. and Lopez-Berestein, G. (1987) Antimicrob. Ag. Chemother. 31, 1901–1903.
[5] Milhaud, J., Hartmann, M.A. and Bolard, J. (1989) Biochimie 71, 49–56.
[6] Milhaud, J., Mazerski, J. and Bolard, J. (1989) Biochim. Biophys. Acta 987, 193–198.
[7] Dufourc, E.J., Smith, I.C.P. and Jarrel, H.C. (1984) Biochim. Biophys. Acta 778, 435–442.
[8] Milhaud, J., Mazerski, J., Bolard, J. and Dufourc, E.J. (1989) Eur. Biophys. J. 17, 151–158.
[9] Hartsel, S.C., Benz, S.K., Peterson, R.P. and Whyte, B.S. (1991) Biochemistry 30, 77–82.
[10] Cohen, B.E. (1992) Biochim. Biophys. Acta 1108, 49–58.
[11] Milhaud, J. (1992) Biochim. Biophys. Acta 1105, 307–318.
[12] Bolard, J. and Milhaud, J. (1996) in Lipids of Pathogenic Fungi (Ghannoun I. and Prasad R., eds.), CRC Press, pp. 254–274.
[13] Morrow, M.R. and Davis, J.H. (1987) Biochim. Biophys. Acta 904, 61–70.
[14] Lewis, R.N.A.H., Mak, N. and McElhaney, R. (1987) Biochemistry 26, 6118–6126.
[15] Finegold, L., Shaw, W.A. and Singer, M.A. (1990) Chem. Phys. Lip. 53, 177–184.
[16] Hatta, I., Matuoka, S., Singer, M.A. and Finegold, L. (1994) Chem. Phys. Lip. 69, 129–136.
[17] Bonev, B. and Morrow, M.R. (1996) Biophys. J. 70, 2727–2735.
[18] Lancelin, J.M. and Beau, J.M. (1989) Tetrahedron Lett. 30, 4521–4524.
[19] Michel, G.W. (1977) in Analytical profiles of drug substances (K. Florey, ed.), Vol. 6, Academic Press, pp. 342–421.
[20] Stewart, J.C.M. (1980) Anal. Biochem. 104, 10–14.
[21] Privalov, P.L. (1980) Pure Appl. Chem. 52, 479–497.
[22] Davis, J.H. (1979) Biophys. J. 27, 339–358.
[23] Davis, J.H. (1983) Biochim. Biophys. Acta 737, 117–171.
[24] Bloom, M., Davis, J.H. and Mackay, A.L. (1981) Chem. Phys. Lett. 80, 198–202.
[25] Sternin, E., Bloom, M. and MacKay, A.L. (1983) J. Magn. Res. 55, 274–282.
[26] Ganis, P., Avitabile, G., Mechlinski, W. and Schaffner, C.P. (1971) J. Am. Chem. Soc. 93, 4560–4564.
[27] Prandi, J. and Beau, J.M. (1989) Tetrahedron Lett. 30, 4517–4520.
[28] Lancelin, J.M., Paquet, F. and Beau, J.M. (1988) Tetrahedron Lett. 29, 2827–2830.
[29] Mazerski, J., Bolard, J. and Borowski, E. (1982) Biochim. Biophys. Acta 719, 11–17.
[30] Cheron, M. (1984) Thèse d'état, Paris VI.
[31] Bittman, R., Chen, W.C. and Blau, L. (1974) Biochemistry 13, 1374–1379.
[32] Connors, K.A. (1987) Binding constants. The Measurement of Molecular Complex Stability. Wiley Interscience, New York, pp. 46–65.
[33] Connors, K.A. (1987) Binding constants. The measurement of molecular complex stability. Wiley Interscience, New York, pp. 26–27.
[34] Cevc, G. and Marsh, D. (1987) Phospholipid bilayers. Physical Principles and Models, Wiley Interscience, New York, pp. 370–377.
[35] Seelig, J. (1977) Q. Rev. Biophys. 10, 353–418.
[36] Léonard, A., Maillet, J.C., Dufourcq, J. and Dufourc, E.J. (1992) Progr. Colloid Sci. 89, 315–318.
[37] Petersen, N.O., Gratton, R. and Pisters, E.M. (1987) Can. J. Chem. 65, 238–244.
[38] Coutinho, A. and Prieto, M. (1995) Biophys. J. 69, 2541–2557.
[39] Arnold, K., Herrmann, A., Garwisch, K. and Pratsch, L. (1987) in Molecular Mechanisms of Membrane Fusion (1987) Plenum, New York, pp. 255–272.
[40] Milhaud, J., Lancelin, J.M., Michels, B. and Blume, A. (1996) Biochim. Biophys. Acta 1278, 223–232.
[41] Grant, C.W.M., Hamilton, K.D. and Barber, K.R. (1989) Biochim. Biophys. Acta 984, 11–20.
[42] Hamilton, K.S., Barber, K.R., Davis, J.H., Neil, K. and Grant, C.W.M. (1991) Biochim. Biophys. Acta 1062, 220–226.